

Table 1. Atlas mouse cDNA expression array (Clontech) results

Experimental		Control		Ratio	Difference	UP	DOWN	Gene	Genbank no.
A1-	VS	O-	O-						
Spot Intensity									
Coordinate	O-	A1-	O-	Ratio	Difference	UP	DOWN	Gene	Genbank no.
D4k	0	7830		N/C	-7830	UP		Interferon inducible protein 1	U19119
D3l	194	5724		29.51	-5530	UP		HMG-box transcription factor from testis (MusSox17)	D49474
F7n	1312	12118		9.24	-10806	UP		Tissue inhibitor of metalloproteinases 3 (TIMP3); SUN	L19622
F7m	1538	7758		5.04	-6220	UP		Tissue inhibitor of metalloproteinases 2 (TIMP2)	X62622
C3h	2237	10392		4.65	-8155	UP		FLICE-like inhibitory protein long form (FLIP-L)	U97076
A4g	1301	5912		4.54	-4611	UP		Ski protooncogene	U14173
A7m	20965	12092		0.58	8873		DOWN	Prothymosin alpha (PTMA)	X56135
B1b	8176	4402		0.54	3774		DOWN	HSP60	X53584
B1d	11509	5186		0.45	6323		DOWN	HSP86; heat shock 86-kDa protein	M36830
F4g	11315	5012		0.44	6303		DOWN	Transforming growth factor beta 2 precursor (TGF-beta 2)	X57413
A1c	6224	2730		0.44	3494		DOWN	Breast cancer type 2 susceptibility protein (BRCA2)	U65594
C1m	7286	3096		0.42	4190		DOWN	Glutathione reductase	X76341
F7a	12115	4714		0.39	7401		DOWN	Interleukin-converting enzyme (ICE)	L28095
B6a	13899	4406		0.32	9493		DOWN	MAP kinase kinase 1	L02526
Spot Intensity									
Coordinate	A1-	A1+	VS	Ratio	Difference	UP	DOWN	Gene	Genbank no.
A1g	9784	997		9.81	-8787		DOWN	Mothers against dpp protein 1 (msMAD1; mSMAD1; MADH1); TGF-beta signaling protein 1 (BSP1)	U58992
B4a	8622	890		9.69	-7732		DOWN	NF-kappa-B transcription factor p65 subunit (NF-kB p65); relA; NFKB3	M61909
E3d	12134	1415		8.58	-10719		DOWN	Interleukin-3 receptor	M29855
E3h	5924	1014		5.84	-4910		DOWN	Interleukin-8 receptor	D17630
F3k	9742	1860		5.24	-7882		DOWN	7S Nerve growth factor alpha subunit (alpha-NGF; NGFA); KLIK4	M11434

F7l	Experimental		VS	Control		UP	DOWN	Gene	Genbank no.
	O+	O-		O+	O-				
F7l	12804	2914	4.39	-9890		DOWN		47-kDa Heat shock protein precursor (HSP47); collagen-binding protein 1 (CBP1); serine protease inhibitor J6	J05609
E3f	23780	6790	3.50	-16990		DOWN		Interleukin-5 receptor alpha subunit precursor (IL-5R alpha)	D90205
C3h	10392	3185	3.26	-7207		DOWN		FLICE-like inhibitory protein long form (FLIP-L)	U97076
D3l	6392	2700	2.37	-3692		DOWN		HMG-box transcription factor from testis (MusSox17)	D49474
F7n	12118	5446	2.23	-6672	UP	DOWN		Tissue inhibitor of metalloproteinases 3 (TIMP3); SUN	L19622
B5l	1182	4778	0.25	3596	UP			58-kDa Inhibitor of RNA-activated protein kinase	U28423
D6h	1500	7089	0.21	5589	UP			T-Lymphocyte activated protein	M31042
C2e	424	4561	0.09	4137	UP			Tumor necrosis factor alpha-induced protein 3 (TNFAIP3); TNFIP3; A20 zinc finger protein	U19463
Control									
O+ VS O-									
Spot intensity									
Coordinate	O-	O+	Ratio	Difference		UP	DOWN	Gene	Genbank no.
D5m	8545	0	N/C	-8545			DOWN	Split hand/foot gene	U41626
D6n	7025	0	N/C	-7025			DOWN	cAMP-Dependent transcription factor 3 (ATF3); activating factor 3; transcription factor LRG-21	U19118
D6m	5215	0	N/C	-5215			DOWN	Transcription factor LIM-1	Z27410
B1d	7205	864	8.34	-6341			DOWN	HSP86; heat shock 86-kDa protein	M36830
B4a	5790	874	6.62	-4916			DOWN	NF-kappa-B transcription factor p65 subunit (NF-kB p65); relA; NFKB3	M61909
F7l	6700	2020	3.32	-4680			DOWN	47-kDa Heat shock protein precursor (HSP47); collagen-binding protein 1 (CBP1); serine protease inhibitor J6	J05609
B6a	8700	2786	3.12	-5914			DOWN	Dual-specificity mitogen-activated protein kinase 1 (MAP kinase kinase 1; MAPK kinase 1; MAPKK1); erk activator kinase 1 (MEK1); PRKMK1	L02526
F7a	7584	2460	3.08	-5124			DOWN	Interleukin-converting enzyme (ICE)	L28095
D1n	1628	9729	0.17	8101	UP			Sim transcription factor	U42554
B5l	1182	7497	0.16	6315	UP			58-kDa Inhibitor of RNA-activated protein kinase	U28423
F7d	1093	8084	0.14	6991	UP			Protease nexin 1 (PN-1)	X70296
D6m	0	8331	0.00	8331	UP			Transcription factor LIM-1	Z27410

The ratio of each pair was calculated with signal intensity, and if the ratio was more than 1.67 or less than 0.6, the spotted genes were considered to be upregulated or downregulated, respectively. Minus sign (-) indicates the absence of AA and β GP and (+) indicates the presence of AA and β GP.

Table 2. Mouse GEM array (Incite/Genome Systems) results: sorted by balanced differential expression in descending order

Differential expression	Kusa-A1 signal	Kusa-O signal	Gene name
5.1	18153	3573	Tissue inhibitor of metalloproteinase 3 (IMAGE:580753)
4.4	2254	516	Myocyte enhancer factor 2C (IMAGE:777101)
3.8	6829	1778	Alkaline phosphatase 2, liver (IMAGE:535409)
3.6	1963	542	ESTs (IMAGE:735883)
3.3	12133	3631	Tenascin C (IMAGE:736372)
3.3	803	241	<i>Mus musculus</i> neural precursor cell expressed developmentally; downregulated Nedd9 (Nedd9) mRNA, complete cds (IMAGE:404536)
2.9	15184	5181	Procollagen, type V, alpha 2 (IMAGE:467107)
2.8	8897	3222	Procollagen, type V, alpha 2 (IMAGE:445075)
2.6	1071	409	ESTs (IMAGE:597280)
2.5	3927	1544	ESTs (IMAGE:419146)
2.5	1683	667	ESTs (IMAGE:479709) ^a
2.4	5265	2152	Procollagen, type XI, alpha 1 (IMAGE:423028)
2.4	2616	1069	Public domain EST (IMAGE:597342)
2.3	6241	2702	Public domain EST (IMAGE:439362)
2.3	1737	749	Kinesin family member 5B (IMAGE:760837)
2.3	829	362	<i>Mus musculus</i> major histocompatibility complex region NG27, NG28, RPS28, NADH oxidoreductase, NG29, KIFC1, Fas-binding protein, BING1, tapasin, RalGDS-like, KE2, BING4, beta 1,3-galactosyl transferase, and RPS18 genes, complete cds (IMAGE:329741)
2.3	2778	1226	Sprouty homolog 1 (<i>Drosophila</i>) (IMAGE:425005)
2.2	2866	1314	ESTs (IMAGE:466255)
2.2	2214	1006	ESTs, weakly similar to plexin 1 (<i>M. musculus</i>) (IMAGE:735903)
2.2	1339	609	Adducin 3 (gamma) (IMAGE:620815)
2.2	5249	2434	Alkaline phosphatase 2, liver (IMAGE:465052)

^aIMAGE:479709 clone was similar to *Mus musculus* MADS box transcription enhancer factor 2, polypeptide C (myocyte enhancer factor 2C)

Table 3. Mouse GEM array (Incite/Genome Systems) results: sorted by balanced differential expression in ascending order

Differential expression	Kusa-A1 signal	Kusa-O signal	Gene name
-5.3	951	5080	Stromal cell-derived factor 1 (IMAGE:533003)
-4.5	205	929	ESTs (IMAGE:779168)
-4.5	156	708	ESTs, weakly similar to cDNA EST EMBL:D75506 comes from this gene (<i>C.elegans</i>) (IMAGE:334182)
-4.4	220	963	ESTs (IMAGE:445426)
-4	1303	5260	Secreted phosphoprotein 1 (IMAGE:571759)
-3.9	362	1408	Four and a half LIM domains 1 (IMAGE:477066)
-3.7	456	1671	Fibrillin 2 (IMAGE:617885)
-3.7	218	809	Complement component 1, r subcomponent (IMAGE:617816)
-3.6	830	3021	<i>Mus musculus</i> OSF-2/periostin mRNA, complete cds (IMAGE:403071) ^a
-3.4	1204	4149	ESTs (IMAGE:617992)
-3.3	324	1060	Complement component 1 subcomponent (IMAGE:676176)
-3	507	1535	Calpain 6 (IMAGE:478504)
-2.9	812	2315	<i>Mus musculus</i> mRNA for dickkopf-3 (dkk-3 gene) (IMAGE:536577)
-2.8	1076	3010	Phosphodiesterase 7A (IMAGE:314384)
-2.8	366	1007	Public domain EST (IMAGE:314509)
-2.7	731	1939	ESTs (IMAGE:536526)
-2.6	1044	2672	Chloride channel 2 (IMAGE:407704)
-2.6	291	768	ESTs, weakly similar to proline-rich protein MP4 (<i>M. musculus</i>) (IMAGE:458992)
-2.6	274	708	Insulin-like growth factor 1 (IMAGE:313322)
-2.5	2177	5462	ESTs, weakly similar to similarity to yeast D-lactate dehydrogenase (<i>C.elegans</i>) (IMAGE:748228)
-2.5	280	693	Public domain EST (IMAGE:479159)
-2.4	2279	5428	Procollagen, type VI, alpha 1 (IMAGE:334132)
-2.4	992	2350	ESTs, highly similar to hypothetical 25.7-kD protein in MSH1-EPT1 intergenic region (<i>Saccharomyces cerevisiae</i>) (IMAGE:337654)
-2.4	329	787	Public domain EST (IMAGE:338162)

^a Periostin, originally called OSF-2 (fasciclin I-like), is mainly detected in the periosteum and may play a role in the recruitment and attachment of osteoblast precursors (22)

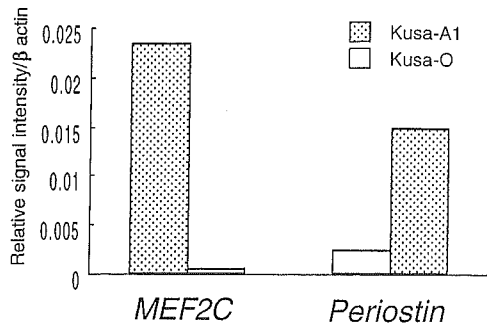


Fig. 7. *MEF2C* and *Periostin* expression in Kusa-A1 (gray bars) and Kusa-O (white bars). Reverse transcription-quantitative polymerase chain reaction (RT-qPCR) confirmed the data obtained by microarray (Table 2). In Kusa-A1, *MEF2C* was highly expressed, but *Periostin* expression was low. On the other hand, in Kusa-O, *MEF2C* expression was low, but *Periostin* expression was high

non-inducing condition, neither of these cell lines exhibited calcium deposits. These results imply that the recruitment of inorganic phosphate by ALP is a necessary but not sufficient condition to induce calcium deposition.

The differential expression of the osteogenic markers, *osteocalcin* and *osteopontin*, in Kusa-A1 and Kusa-O indicates their stage of osteogenesis. Osteocalcin, a kind of bone “gla” (gamma carboxy-glutamic acid) protein (BGP), is the major non-collagenous extracellular protein of bone tissue, and is thought to play an important role in bone mineral deposition with its gamma carboxy-glutamic acid residues [25]. *Osteopontin* is another osteogenic marker expressed in the middle stage of osteoblast differentiation in vitro. In this study, Kusa-A1 showed osteocalcin expression within 1 day after confluency in the inducing condition and 5 days after confluency in the non-inducing condition. But Kusa-O did not exhibit osteocalcin expression in either the inducing condition or the non-inducing condition. On the other hand, *osteopontin* expression was rather constant through the experimental time course in Kusa-O, but was high only in the inducing condition in Kusa-A1. To summarize these results, Kusa-A1 could be classified as a more mature stage of osteoblast than Kusa-O, a classification which is compatible with their osteogenesis/mineralization abilities in vivo and in vitro.

For Kusa-A1, some specific conditions have induced its differentiation into various types of cells. For example, Makino et al. [5] showed that Kusa-A1 differentiated into adipocytes or myotubes with 5-aza cytidine treatment. Moreover, the introduction of noggin, a suppressor of bone morphogenic protein (BMP) induced active neurons from Kusa-A1 [8]. These results indicate that Kusa should be considered as a kind of stem cell or progenitor cell, not as a simple osteoblastic cell line. We examined the expression of Notch signal-related genes that could be important for the regulation of various types of stem/progenitor cells. Notch signaling in stem cells models is often demonstrated as lateral inhibition or lateral specification [26,27]. These models well explain the “salt-and-pepper pattern” seen in the differentiation of stem cells [28], in which an active Notch

signal creates reciprocal patterns in neighboring cells. Our high-magnification view of calcified deposits in Kusa-A1 indicated this salt-and-pepper-like pattern, which may correspond to an activated Notch signal. In contrast, the obscure pattern of calcification in Kusa-O may indicate an inactive state of Notch signaling. In fact, our previous study demonstrated that a constitutively active form of Notch1 influenced the osteogenesis/mineralization ability of Kusa [29]. But Northern blot analysis showed that *HES1*, a downstream gene in the Notch signal pathway, changed its expression level only in Kusa-A1, in the non-inducing condition. The Notch signal has many different downstream factors, such as nuclear factor kappaB, p-300, Deltex, and mitogen-activated protein kinase (MAPK), other than the Epstein-Barr virus (EBV) latency C promoter binding factor 1 (CBF1)/hairly and enhancer of split 1 (*HES1*) pathway and employs them differentially. *HES1* may not be involved in the Notch signal pathway of Kusa.

Actually, the analysis of 588 cDNAs is not sufficient to use the term “global”, but, with this small-number microarray, we detected that gross downregulation occurred in the inducing condition in both Kusa-A1 and Kusa-O. This indicates that “master gene expression” is not necessarily associated with osteogenesis/mineralization in Kusa, and conversely, the gross downregulation may carve out specific networks of signal pathways, resulting in the unidirectional differentiation of osteogenesis/mineralization. This hypothesis is a concept that is completely opposite to the “master gene theory”, and further verification with other types of cell lines should be performed to test this hypothesis.

The high-throughput microarray (GEMarray), which was carried on Kusa-A1 and Kusa-O in the non-inducing condition, revealed a relatively high expression of *periostin* in Kusa-O cells. *Periostin* was identified from the screening of MC3T3-E1-specific genes, and sequence similarity analysis has revealed that it is homologous to fasciclin [30], a type of homophilic binding molecule [31,32]. *Periostin* is specifically expressed in the periosteum and the periodontal ligament [24]. The function of *periostin* remains to be elucidated, but recent reports indicate a relationship with cell attachment [33–36]. As compared with Kusa-A1, MC3T3-E1 in the non-inducing condition should be classified as showing a rather immature state of osteogenesis, and Kusa-O should also be included in this category. The high level of expression of *periostin* in MC3T3-E1 and Kusa-O may imply its role in the early stage of osteogenesis, although further investigation remains to be done to specify the molecular basis of this role.

In contrast to *periostin* expression in Kusa-A1, *MEF2C* showed enhanced expression. *MEF2C* is a basic/helix-loop-helix (bHLH) transcriptional factor and is known to be a late-stage regulator of myogenesis, under the control of *MyoD*, *Myf5*, and some other early myogenic genes [37–39]. However, we could not find upregulation of any other myogenic genes with the GEMarray microarray analysis. Recently, further roles and relationships of *MEF2C* have been found, such its action as an apoptotic factor in neurogenesis [40,41] and stem cell regulation, in the context of Notch

signaling, in both vertebrates and invertebrates [42]. As mentioned, it was difficult to find the direct involvement of *HES1* in the Notch pathway of Kusa, though activation of the Notch signal has been shown to suppress the differentiation of Kusa-A1 [29]. The Notch signal seems to employ some pathway(s) other than its classical one, and *MEF2C* could be a candidate. *CCN3* is a positive regulator of the Notch signal and its high expression in Kusa may be related to this kind of non-classical pathway of the Notch signal.

In conclusion, we investigated two sublines of Kusa from several different aspects and clarified their specific characteristics. Kusa seems to be a useful cell line, considering its high osteogenesis/mineralization activity; investigation of the molecular basis of this activity will give new insights for the technical development of osteogenic restitution.

Acknowledgments This work was supported by Grants-in-Aids from the Japanese Society for the Promotion of Science: no. 14370615 to N.K.; and nos. 15390552 and 12671763 to K.K.

References

- Gershon D (2002) Microarray technology: an array of opportunities. *Nature* 416:885–891
- Pittenger MF, Mackay AM, Beck SC, Jaiswal RK, Douglas R, Mosca JD, Moorman MA, Simonetti DW, Craig S, Marshak DR (1999) Multilineage potential of adult human mesenchymal stem cells. *Science* 284:143–147
- Dexter TM, Testa NG (1976) Differentiation and proliferation of hemopoietic cells in culture. *Methods Cell Biol* 14:387–405
- Seale P, Rudnicki MA (2000) A new look at the origin, function, and “stem-cell” status of muscle satellite cells. *Dev Biol* 218:115–124
- Makino S, Fukuda K, Miyoshi S, Konishi F, Kodama H, Pan J, Sano M, Takahashi T, Hori S, Abe H, Hata J, Umezawa A, Ogawa S (1999) Cardiomyocytes can be generated from marrow stromal cells in vitro. *J Clin Invest* 103:697–705
- Umezawa A, Maruyama T, Segawa K, Shaddock RK, Waheed A, Hata J (1992) Multipotent marrow stromal cell line is able to induce hematopoiesis in vivo. *J Cell Physiol* 151:197–205
- Hall FL, Han B, Kundu RK, Yee A, Nimni ME, Gordon EM (2001) Phenotypic differentiation of TGF-beta1-responsive pluripotent pre-mesenchymal prehematopoietic progenitor (P4 stem) cells from murine bone marrow. *J Hematother Stem Cell Res* 10:261–271
- Kohyama J, Abe H, Shimazaki T, Koizumi A, Nakashima K, Gojo S, Taga T, Okano H, Hata J, Umezawa A (2001) Brain from bone: efficient “meta-differentiation” of marrow stroma-derived mature osteoblasts to neurons with Noggin or a demethylating agent. *Differentiation* 68:235–244
- Mitaka T (2001) Hepatic stem cells: from bone marrow cells to hepatocytes. *Biochem Biophys Res Commun* 281:1–5
- Steidl U, Kronenwett R, Rohr UP, Fenk R, Kliszewski S, Maercker C, Neubert P, Aivado M, Koch J, Modlich O, Bojar H, Gattermann N, Haas R (2002) Gene expression profiling identifies significant differences between the molecular phenotypes of bone marrow-derived and circulating human CD34+ hematopoietic stem cells. *Blood* 99:2037–2044
- Sata M, Saiura A, Kunisato A, Tojo A, Okada S, Tokuhisa T, Hirai H, Makuuchi M, Hirata Y, Nagai R (2002) Hematopoietic stem cells differentiate into vascular cells that participate in the pathogenesis of atherosclerosis. *Nat Med* 8:403–409
- Lassar AB, Paterson BM, Weintraub H (1986) Transfection of a DNA locus that mediates the conversion of 10T1/2 fibroblasts to myoblasts. *Cell* 47:649–656
- Weintraub H, Davis R, Tapscott S, Thayer M, Krause M, Benezra R, Blackwell TK, Turner D, Rupp R, Hollenberg S, Zhuang Y, Lassar A (1991) The myoD gene family: nodal point during specification of the muscle cell lineage. *Science* 251:761–766
- Tontonoz P, Hu E, Spiegelman BM (1994) Stimulation of adipogenesis in fibroblasts by PPAR gamma 2, a lipid-activated transcription factor. *Cell* 79:1147–1156
- Komori T, Yagi H, Nomura S, Yamaguchi A, Sasaki K, Deguchi K, Shimizu Y, Bronson RT, Gao YH, Inada M, Sato M, Okamoto R, Kitamura Y, Yoshiki S, Kishimoto T (1997) Targeted disruption of *Cbfa1* results in a complete lack of bone formation owing to maturational arrest of osteoblasts. *Cell* 89:755–764
- Nakashima K, Zhou X, Kunkel G, Zhang Z, Deng JM, Behringer RR, de Crombrughe B (2002) The novel zinc finger-containing transcription factor osterix is required for osteoblast differentiation and bone formation. *Cell* 108:17–29
- Rodan GA, Noda M (1991) Gene expression in osteoblastic cells. *Crit Rev Eukaryot Gene Expr* 1:85–98
- Yasui N, Ochi T, Takaoka K, Ono K, Nakata Y (1980) Osteogenesis by factor(s) isolated from mouse osteosarcoma cells in combination with collagen. *Biken J* 23:83–87
- Chen JJ, Wu R, Yang PC, Huang JY, Sher YP, Han MH, Kao WC, Lee PJ, Chiu TF, Chang F, Chu YW, Wu CW, Peck K (1998) Profiling expression patterns and isolating differentially expressed genes by cDNA microarray system with colorimetry detection. *Genomics* 51:313–324
- Ecarot-Charrier B, Glorieux FH, van der Rest M, Pereira G (1983) Osteoblasts isolated from mouse calvaria initiate matrix mineralization in culture. *J Cell Biol* 96:639–643
- Schoeters GE, de Saint-Georges L, Van den Heuvel R, Vanderborcht O (1988) Mineralization of adult mouse bone marrow in vitro. *Cell Tissue Kinet* 21:363–374
- Celeste AJ, Rosen V, Buecker JL, Kriz R, Wang EA, Wozney JM (1986) Isolation of the human gene for bone gla protein utilizing mouse and rat cDNA clones. *Embo J* 5:1885–1890
- Nomura S, Wills AJ, Edwards DR, Heath JK, Hogan BL (1988) Developmental expression of 2ar (osteopontin) and SPARC (osteonectin) RNA as revealed by in situ hybridization. *J Cell Biol* 106:441–450
- Horiuchi K, Amizuka N, Takeshita S, Takamatsu H, Katsuura M, Ozawa H, Toyama Y, Bonewald LF, Kudo A (1999) Identification and characterization of a novel protein, periostin, with restricted expression to periosteum and periodontal ligament and increased expression by transforming growth factor beta. *J Bone Miner Res* 14:1239–1249
- Boskey AL, Gadaleta S, Gundberg C, Doty SB, Ducy P, Karsenty G (1998) Fourier transform infrared microspectroscopic analysis of bones of osteocalcin-deficient mice provides insight into the function of osteocalcin. *Bone* 23:187–196
- Sternberg PW (1988) Lateral inhibition during vulval induction in *Caenorhabditis elegans*. *Nature* 335:551–554
- Freitas C, Rodrigues S, Charrier JB, Teillet MA, Palmeirim I (2001) Evidence for medial/lateral specification and positional information within the presomitic mesoderm. *Development* 128:5139–5147
- Marnellos G, Deblandre GA, Mjolsness E, Kintner C (2000) Delta-Notch lateral inhibitory patterning in the emergence of ciliated cells in *Xenopus*: experimental observations and a gene network model. *Pac Symp Biocomput* 5:329–340
- Shindo K, Kawashima N, Sakamoto K, Yamaguchi A, Umezawa A, Takagi M, Katsube K, Suda H (2003) Osteogenic differentiation of mesenchymal progenitor cells, Kusa is suppressed by Notch signaling. *Exp Cell Res* 290:370–380
- Takeshita S, Kikuno R, Tezuka K, Amann E (1993) Osteoblast-specific factor 2: cloning of a putative bone adhesion protein with homology with the insect protein fasciclin I. *Biochem J* 294 (Pt 1):271–278
- Elkins T, Hortsch M, Bieber AJ, Snow PM, Goodman CS (1990) *Drosophila* fasciclin I is a novel homophilic adhesion molecule that along with fasciclin III can mediate cell sorting. *J Cell Biol* 110:1825–1832
- Elkins T, Zinn K, McAllister L, Hoffmann FM, Goodman CS (1990) Genetic analysis of a *Drosophila* neural cell adhesion molecule: interaction of fasciclin I and Abelson tyrosine kinase mutations. *Cell* 60:565–575
- Shao R, Bao S, Bai X, Blanchette C, Anderson RM, Dang T, Gishizky ML, Marks JR, Wang XF (2004) Acquired

- expression of periostin by human breast cancers promotes tumor angiogenesis through up-regulation of vascular endothelial growth factor receptor 2 expression. *Mol Cell Biol* 24:3992–4003
34. Nakazawa T, Nakajima A, Seki N, Okawa A, Kato M, Moriya H, Amizuka N, Einhorn TA, Yamazaki M (2004) Gene expression of periostin in the early stage of fracture healing detected by cDNA microarray analysis. *J Orthop Res* 22:520–525
 35. Kudo H, Amizuka N, Araki K, Inohaya K, Kudo A (2004) Zebrafish periostin is required for the adhesion of muscle fiber bundles to the myoseptum and for the differentiation of muscle fibers. *Dev Biol* 267:473–487
 36. Bao S, Ouyang G, Bai X, Huang Z, Ma C, Liu M, Shao R, Anderson RM, Rich JN, Wang XF (2004) Periostin potently promotes metastatic growth of colon cancer by augmenting cell survival via the Akt/PKB pathway. *Cancer Cell* 5:329–339
 37. Takebayashi-Suzuki K, Pauliks LB, Eltsefon Y, Mikawa T (2001) Purkinje fibers of the avian heart express a myogenic transcription factor program distinct from cardiac and skeletal muscle. *Dev Biol* 234:390–401
 38. Sartorelli V, Huang J, Hamamori Y, Kedes L (1997) Molecular mechanisms of myogenic coactivation by p300: direct interaction with the activation domain of MyoD and with the MADS box of MEF2C. *Mol Cell Biol* 17:1010–1026
 39. Edmondson DG, Lyons GE, Martin JF, Olson EN (1994) Mef2 gene expression marks the cardiac and skeletal muscle lineages during mouse embryogenesis. *Development* 120:1251–1263
 40. Okamoto S, Krainc D, Sherman K, Lipton SA (2000) Antiapoptotic role of the p38 mitogen-activated protein kinase-myocyte enhancer factor 2 transcription factor pathway during neuronal differentiation. *Proc Natl Acad Sci U S A* 97:7561–7566
 41. Okamoto S, Li Z, Ju C, Scholzke MN, Mathews E, Cui J, Salvesen GS, Bossy-Wetzel E, Lipton SA (2002) Dominant-interfering forms of MEF2 generated by caspase cleavage contribute to NMDA-induced neuronal apoptosis. *Proc Natl Acad Sci U S A* 99:3974–3979
 42. Wilson-Rawls J, Molkentin JD, Black BL, Olson EN (1999) Activated notch inhibits myogenic activity of the MADS-Box transcription factor myocyte enhancer factor 2C. *Mol Cell Biol* 19:2853–2862

Immortalization of Human Fetal Cells: The Life Span of Umbilical Cord Blood-derived Cells Can Be Prolonged without Manipulating p16^{INK4a}/RB Braking Pathway[□]

Masanori Terai,*[†] Taro Uyama,* Tadashi Sugiki,* Xiao-Kang Li,[‡]
Akihiro Umezawa,*[§] and Tohru Kiyono[†]

Departments of *Reproductive Biology and Pathology and [†]Innovative Surgery, National Research Institute for Child Health and Development, Tokyo 157-8535, Japan; [‡]Virology Division, National Cancer Center Research Institute, Tokyo, Japan; and [§]Department of Pathology, Keio University School of Medicine, Tokyo 160-8582, Japan

Submitted July 31, 2004; Accepted December 20, 2004
Monitoring Editor: Lawrence Goldstein

Human umbilical cord blood-derived mesenchymal stem cells (UCBMSCs) are expected to serve as an excellent alternative to bone marrow-derived human mesenchymal stem cells. However, it is difficult to study them because of their limited life span. To overcome this problem, we attempted to produce a strain of UCBMSCs with a long life span and to investigate whether the strain could maintain phenotypes in vitro. UCBMSCs were infected with retrovirus carrying the human telomerase reverse transcriptase (hTERT) to prolong their life span. The UCBMSCs underwent 30 population doublings (PDs) and stopped dividing at PD 37. The UCBMSCs newly established with hTERT (UCBTERTs) proliferated for >120 PDs. The p16^{INK4a}/RB braking pathway leading to senescence can be inhibited by introduction of Bmi-1, a polycomb-group gene, and human papillomavirus type 16 E7, but the extension of the life span of the UCBMSCs with hTERT did not require inhibition of the p16^{INK4a}/RB pathway. The characteristics of the UCBTERTs remained unchanged during the prolongation of life span. UCBTERTs provide a powerful model for further study of cellular senescence and for future application to cell-based therapy by using umbilical cord blood cells.

INTRODUCTION

Human mesenchymal stem cells (hMSCs) can be a useful source of cells for transplantation for several reasons: they have the ability to proliferate and differentiate into mesodermal tissues, and they entail no ethical or immunological problems (Caplan, 1991; Prockop, 1997; Caplan and Bruder, 2001). hMSCs have been studied extensively over the past 3 decades, and numerous independent research groups have successfully isolated hMSCs from a variety of sources, most commonly, from the bone marrow (Owen, 1988; Umezawa *et al.*, 1992; Jaiswal *et al.*, 1997; Makino *et al.*, 1999; Pittenger *et al.*, 1999; Sekiya *et al.*, 2004). Umbilical cord blood (UCB) contains circulating stem/progenitor cells, and the cells contained in UCB are known to be distinct from those contained in bone marrow and adult peripheral blood (Mayani and Lansdorp, 1998). Isolation, characterization, and differentiation of clonally expanded hMSCs derived from UCB (UCBMSCs) have been reported (Goodwin *et al.*, 2001; Lee *et al.*, 2004), and UCBMSCs have been found to have multipotency, and the immunophenotype of the clonally expanded cells is consistent with that reported for bone marrow mes-

enchymal stem cells. Even now, most UCB is regarded as medical waste in the delivery rooms. Aspirating bone marrow from patients is, however, an invasive procedure, and the proliferation and differentiation capacity of hMSCs decreases with the donor age (D'Ippolito *et al.*, 1999). Therefore, the applications of UCB should be further expanded.

UCBMSCs will be useful sources for cell transplantation, however, it is difficult to study and apply them because of their limited life span. One of the reasons for this is that normal human cells undergo a limited number of cell division in culture and then enter a nondividing state called "senescence" (Hayflick, 1976; Campisi, 1997). Human cells reach senescence or cease to divide after a limited number of cell replications, and the average number of hMSC population doublings (PDs) has been found to be ~40 (Takeda *et al.*, 2004), implying that it would be difficult to obtain enough cells to restore the function of a failing human organ. Large numbers of cells must be injected into damaged tissues to restore function in humans, and cells sometimes need to be injected throughout entire organs.

To resolve these problems, the life span of hMSCs from bone marrow can be extended by retroviral transduction of human telomerase reverse transcriptase (hTERT) (Blackburn, 2000a,b, 2001) and human papillomavirus type 16 (HPV16) E6 and/or E7 (Sekiguchi *et al.*, 1999; Burk *et al.*, 2003; Takeda *et al.*, 2004). Both p16^{INK4a}/RB inactivation with E7 and telomerase activation with E6 are required to extend the life span of human mammary epithelial cells (Kiyono *et al.*, 1998). E6 also accelerates degradation of p53, which induces the cdk inhibitor p21 (Sekiguchi and Hunter, 1998). This system in which p16^{INK4a}/RB is inhibited and

This article was published online ahead of print in *MBC in Press* (<http://www.molbiolcell.org/cgi/doi/10.1091/mbc.E04-07-0652>) on January 12, 2005.

[□] The online version of this article contains supplemental material at *MBC Online* (<http://www.molbiolcell.org>).

Address correspondence to: Akihiro Umezawa (umezawa@1985.jukuin.keio.ac.jp).

telomerase is activated is highly efficient in extending the life span of hMSCs (Okamoto *et al.*, 2002).

In the present study, we investigated the growth regulatory mechanism of UCBMSCs and attempted to establish UCBMSCs with hTERT (UCBTERTs) to overcome their limited life span. Introduction of hTERT alone was sufficient to extend the life span of UCBMSCs *in vitro*, and this technique for prolonging the life span of UCBMSCs will be a useful tool. UCBTERTs with the extended life span provide a powerful model for further study of cellular senescence and application to transplantation therapy in the future.

MATERIALS AND METHODS

Isolation and Cell Culture of UCBMSCs

UCB was collected on delivery with informed consent. UCB mononuclear cells were obtained as per the manufacturer's instructions, followed by Ficoll-Paque (Amersham Biosciences, Piscataway, NJ) density gradient centrifugation (1.077 g/cm³), and plated in tissue culture dishes (BD Biosciences, San Jose, CA) in DMEM medium (Sigma-Aldrich, St. Louis, MO) and 10% fetal bovine serum (FBS) (Vitromex, Geilenkirchen, Germany). All cultures were maintained at 37°C in a humidified atmosphere containing 95% air and 5% CO₂. A few colonies were found in the culture dish 1 mo after the collected cells were cultured in DMEM with 10% FBS. One colony was trypsinized using a colony cylinder and then diluted and plated on 12-well plates (BD Biosciences) in mesenchymal stem cell growth medium (MSCGM, PT-3001; Cambrex Bio Science Walkersville, Walkersville, MD) at a final density of $\sim 4 \times 10^5$ cells/well in a 12-well plate. MSCGM was used in all culture procedures after harvesting the colony. The cells were passaged at a density of $\sim 1 \times 10^5$ cells/100-mm dish (1:4), and the original cells were regarded as being PD 0 (day 0). When the cultures reached subconfluence, the cells were harvested with 0.25% trypsin and 1 mM EDTA and replated with one-half of the harvested cells. Cells were allowed to adhere overnight, and nonadherent cells were washed out with medium changes. Medium changes were carried out twice weekly thereafter. The cells were cultured for further experiments under the approval (approval nos. 7 and 55) of the Ethics Committee of National Research Institute for Child Health and Development, Tokyo.

Infection with Recombinant Retroviruses

The cells were prepared for infection with recombinant retroviruses expressing the E6, E7, and hTERT, as described previously (Takeda *et al.*, 2004). Stably transduced cells with an expanded life span were designated UCBE6E7-20 and UCBTERT-21 cells.

Senescence-associated- β -gal (SA- β -gal) Staining

The SA- β -gal assay was performed as described previously (Dimiri *et al.*, 1995). Cells were washed in phosphate-buffered saline (PBS), fixed for 3–5 min at room temperature in 2% formaldehyde/0.2% glutaraldehyde (or 3% formaldehyde), washed, and incubated at 37°C with fresh SA- β -gal stain solution: 1 mg of 5-bromo-4-chloro-3-indolyl β -D-galactosidase per milliliter (stock is 20 mg of dimethylformamide/ml), 40 mM citric acid/sodium phosphate, pH 6.0, 5 mM potassium ferrocyanide, 5 mM potassium ferricyanide, 150 mM NaCl, and 2 mM MgCl₂. Staining was evident in 2–4 h and maximal in 12–16 h.

Cell Transplantation

Freshly collected confluent cells (10⁶ cells) were subcutaneously and intramuscularly injected into BALB/c nu/nu mice (Sankyo Laboratory, Hamamatsu, Japan). Animals were monitored for malignant transformation of the injected cells for 3 mo after inoculation and then killed by cervical location.

Flow Cytometric Analysis

Cells were stained for 30 min at 4°C with primary antibodies and immunofluorescent secondary antibodies. The cells were then analyzed on a FACScan (BD Biosciences), and the data were analyzed with the CELLQUEST software (BD Biosciences). Antibodies against human CD13, CD14, CD29, CD31, CD34, CD44, CD45, CD50, CD55, CD59, CD90, CD117, and CD133 were purchased from Beckman Coulter (Fullerton, CA), Immunotech (Marseille, France), Cytotech (Hellebaek, Denmark), and BD Biosciences PharMingen (San Diego, CA).

Western Blot Analysis

Cells were seeded at a density of 3×10^5 cells/100-mm culture dish and harvested at subconfluence. Cell lysates were prepared by sonication by using ultrasonic homogenizer VP-5S in WE16th lysis buffer (Gewin *et al.*, 2004). Equal amounts of protein (20 μ g) were loaded on SDS-polyacrylamide gels

and blotted on Immobilon-P membranes (Millipore, Bedford, MA) by using a semidry transfer system (Atto, Tokyo, Japan). The primary antibodies used were as follows: G3-245 for retinoblastoma (RB) protein and G175-405 for p16^{INK4a} (BD Biosciences PharMingen), DO-1 for p53 (Oncogene Science, Cambridge, MA), F-5 for p21 and I-19 for actin (Santa Cruz Biotechnology, Santa Cruz, CA), affinity-purified anti-phospho-ataxia telangiectasia mutated kinase (p-ATM) (Ser1981) (600-401-400; Rockland, Gilbertsville, PA), and phospho-p53 (p-p53) (Ser15) antibody (9284; Cell Signaling Technology, Beverly, MA). Blots were probed with horseradish peroxidase-conjugated goat anti-mouse IgG (Jackson ImmunoResearch Laboratories, West Grove, PA), anti-rabbit IgG (New England Biolabs, Beverly, MA), or donkey anti-goat IgG (Santa Cruz Biotechnology), and visualized using an enhanced chemiluminescence detection kit (Roche Diagnostics, Indianapolis, IN).

Telomere Length Assay

Total genomic DNA was isolated from cultured cells by proteinase K digestion. The lengths of telomere in each sample were determined by Southern blot analysis as described previously (Vaziri *et al.*, 1994). Briefly, 1 μ g of genomic DNA extracted from each sample was digested with both *Hinf*I and *Rsa*I and electrophoresed in 0.8% agarose gels for 16 h, transferred onto a Hybond N membrane (Amersham Biosciences), and hybridized with digoxigenin (DIG)-labeled (TTAGGG)₃ probe. The membrane was incubated with anti-DIG alkaline phosphatase (ALP) antibody, and detection was performed with chemiluminescence solution.

Telomerase Activity

Telomerase activity in each sample was detected by the telomeric repeat amplification protocol (TRAP) assay by using the TRAPEze kit (Intergen, Purchase, NY) according to the manufacturer's instruction.

Karyotype Analysis

Fixation and chromosome preparation were performed according to the standard procedure described previously (Sasaki, 1975). For each sample, >50 cells were scored for their chromosome number.

Differentiation-Induction Experiments

The multidirectional differentiation potential of each cell line was assessed by the differentiation-induction protocols described below.

Histochemical Staining

After 21 d of culture, cells were rinsed twice with PBS and then fixed with 10% buffered formalin for 10 min at room temperature. The fixed cells were stained with 0.3% Oil-Red-O (Nakarai Tesque, Kyoto, Japan) for the adipogenic differentiation assay and with 5% silver nitrate (Nakarai Tesque) for von Kossa staining in the osteogenic differentiation assay (Tsuchiya *et al.*, 2004).

Osteogenic Differentiation

Cells were seeded at a density of 5×10^4 cells/cm² in tissue culture dishes and cultured with MSCGM containing 100 nM dexamethasone, 50 μ M ascorbic acid 2-phosphate, and β -glycerophosphate. The cultures were maintained for 4 wk, and the cultured medium was replaced every 3 d.

Adipogenic Differentiation

Cells were seeded at a density of 3×10^4 cells/cm² in tissue culture dishes. When the cells were confluent, the adipogenic differentiation was initiated by three cycles of induction/maintenance culture. Each cycle consists of 3 d of culture in the induction medium (DMEM with 10% FBS, 1 μ M dexamethasone, 0.2 mM indomethacin, 10 μ g/ml insulin, and 0.5 mM 3-isobutyl-1-methylxanthine) followed by 2 d of culture in the maintenance medium (DMEM with 10% FBS and 10 μ g/ml insulin).

RESULTS

Establishment of UCB-derived Cells with an Extended Life Span

UCBMSCs regarded as being PD 0, or day 0, were fibroblast-like in morphology, indistinguishable in appearance from the marrow-derived MSCs, and relatively larger in size than rapidly self-renewing stem cells (Prockop *et al.*, 2001) and multipotent adult progenitor stem cells (Jiang *et al.*, 2002) (Figure 1A). The cells from PD 9 to PD 31 rapidly proliferated in culture, and propagated continuously (Figure 1, B and C). No SA- β -gal activity was detected histoenzymologically in the UCBMSCs in the growth phase on day 59. The UCBMSCs stopped replicating, became broad and flat, and exhibited SA- β -gal activity as indicated by blue staining of

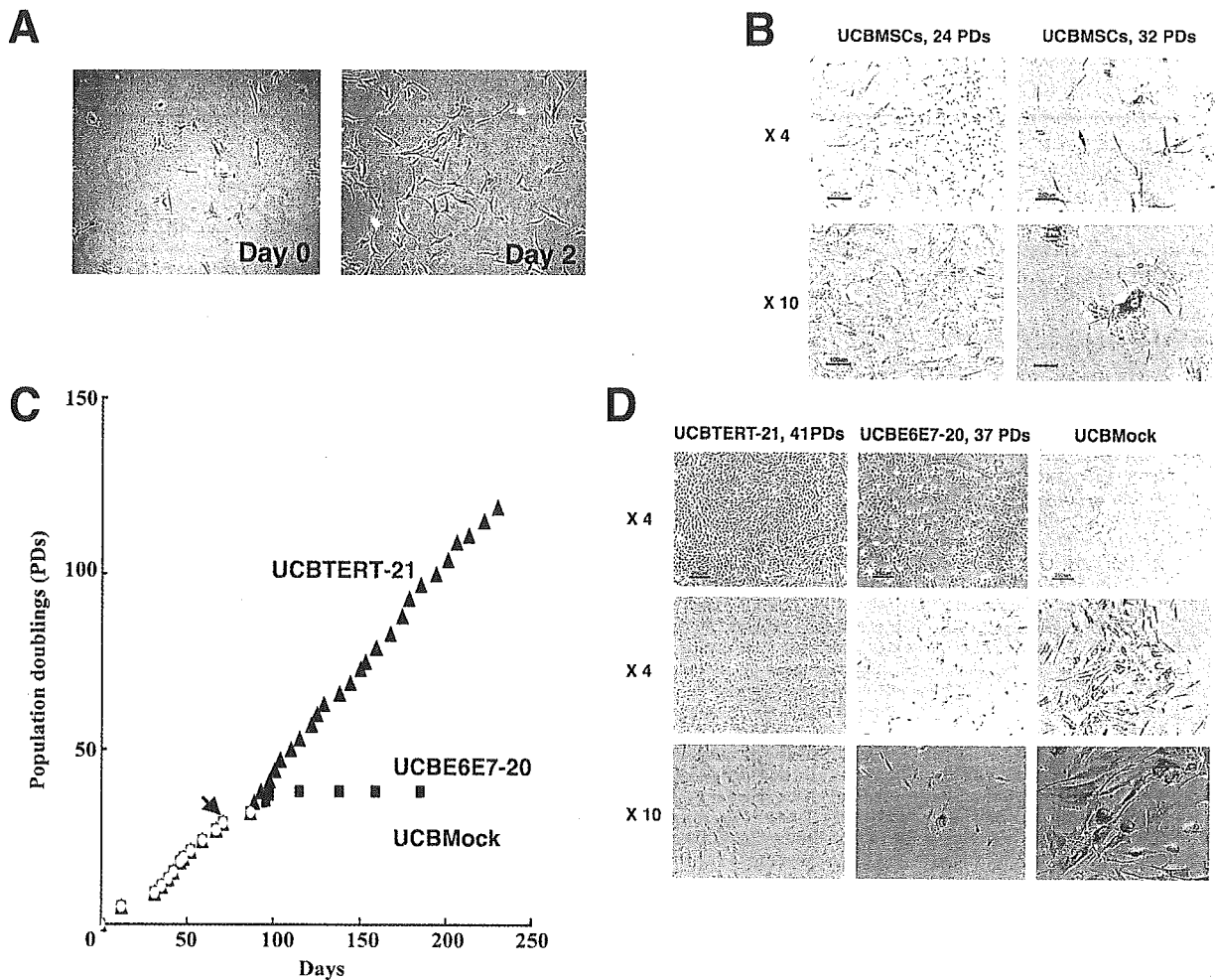
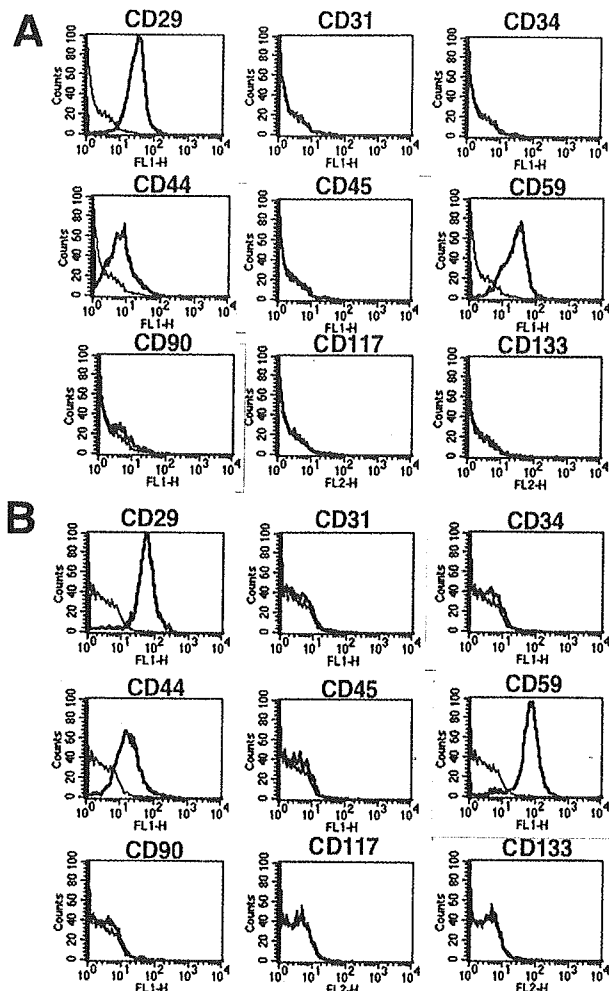


Figure 1. In vitro growth and SA- β -gal activity of UCBMSCs, UCBE6E7-20 cells, and UCBTERT-21 cells. (A) Morphology of human UCBMSCs (left, day 0; right, day 2; original magnification, 10 \times). (B) Morphological changes and SA- β -gal activity of UCBMSCs. UCBMSCs were a broad and flat, ceased to proliferate, and exhibited high SA- β -gal activity as indicated by their cytoplasm staining blue at PD 32 (14 passages at day 98), suggesting senescence. No SA- β -gal activity was detected in the UCBMSCs in the growth phase at PD 24 (10 passages at day 59 in left column). Bar, 250 μ m in the upper column and 100 μ m in the lower column. (C) Population doublings of UCBMock cells (yellow circles), UCBE6E7-20 cells (red squares), and UCBTERT-21 cells (blue triangles) are shown. UCBMSCs were infected with recombinant retroviruses carrying E6 and E7 or hTERT or were treated with polybrene alone at PD 29 (indicated as an arrow). UCBTERT-21 cells proliferated for >120 PDs and for >250 d and exhibited persistent growth. UCBE6E7-20 cells exhibited a prolonged cell life span in culture, reached 38 PDs, and then entered crisis. UCBMock cells stopped growing and entered senescence at 32 PDs. (D) Morphological changes (top column) and SA- β -gal activity (middle and bottom column) of UCBMock cells, UCBE6E7-20 cells, and UCBTERT-21 cells. No staining was detected in UCBTERT-21 cells at PD 41 (left column, 16 passages at day 98) with the SA- β -gal stain (middle and bottom columns). A few UCBE6E7 cells were positive with SA- β -gal stain at PD 37 (middle column, 15 passages at day 98). UCBMock cells were broad and flat at PD 32 (right column, 14 passage at day 98), indicating senescence.

their cytoplasm at PD 32 or day 98, indicating that they had entered senescence (Figure 1, B and C). The morphological changes and SA- β -gal activity of UCBMSCs are PD dependent. To extend the cells' life span and obtain a large number of cells, two different types of cells were obtained by transferring a combination of HPV16 E6 and E7 or hTERT at 29 PDs or 12 passages (Figure 1C, indicated as an arrow). UCBMSCs transduced with a combination of E6 and E7 were designated UCBE6E7-20 cells, and UCBMSCs transduced with hTERT were named UCBTERT-21 cells. UCBTERT-21 cells successfully proliferated >120 PDs, and continued to grow. The cells were found to have an extended life span (Figure 1C, UCBTERT-21 cells, blue triangles). The UCBE6E7-20 cells, which had been transduced with E6 and E7, had a prolonged cell life span in culture, and underwent global cell death at 38 PDs,

when the cells entered a "crisis" period. This implies that the E6 and E7 are capable of prolonging cell life span but that their effect is limited (Figure 1C, UCBE6E7-20 cells, pink squares). Mock infection (polybrene treatment alone) did not extend cell life span, and the cells reached senescence or cessation of growth at PD 32 (Figure 1C, UCBMock, yellow circles). SA- β -gal staining was performed to determine the proportions of cells that had entered senescence, and positive staining was observed in 0% of the UCBTERT-21 cells at PD 41, 2% of the UCBE6E7-20 cells at PD 37, and 100% of the UCBMock cells at PD 32 (Figure 1D). The low percentage of SA- β -gal-positive UCBE6E7-20 cells at PD 37 or day 98 is probably attributable to global cell death by crisis (Figure 1D, middle column). UCBMock cells exhibited a typical senescence-associated morphology, i.e., they were broad and flat and exhibited strong SA- β -



Surface marker	UCBMSCs	UCBTERT-21
CD34	-	-
CD117	-	-
CD31	-	-
CD13	-	-
CD14	-	-
CD29	+++	+++
CD44	++	++
CD45	-	-
CD50	-	-
CD55	++	++
CD59	+++	+++
CD90	-	-
CD133	-	-

Figure 2. Flow cytometric analysis of cell surface markers of UCBMSCs and UCBTERT-21 cells. UCBMSCs (A) displayed the same pattern of surface markers as UCBTERT-21 cells (B). No difference in cell surface markers was found between UCBMSCs and UCBTERT-21 cells as summarized in the table (C). Both were positive for CD29 (integrin β 1), CD44 (Pgp-1/ly-24), and CD59, and negative for CD31 (PECAM-1), CD34, CD45 (leukocyte common antigen), CD90 (Thy-1), CD117 (c-kit), and CD133.

gal activity enzyme cytochemically at PD 32 (Figure 1D, right column).

The cells did not undergo malignant transformation. They stopped dividing after reaching confluence, and they did not form any foci after confluence in vitro. Nor did the cells grafted into the subcutaneous and muscle tissue of nude mice ($n = 6$) produce tumors, at least during the monitoring period (>100 d). Injected UCBTERT-21 cells survived but did not proliferate at the injection sites.

Unchanged Surface Markers of UCBMSCs after Prolongation of Their Life Span

Expression of UCBMSCs and UCBTERT-21 cell surface markers was evaluated by flow cytometric analysis (Figure 2). The results showed that both cells were positive for CD29 (integrin β 1), CD44 (Pgp-1/ly-24), CD55, and CD59, and negative for CD13, CD14 (a marker for macrophages and dendritic cells), CD31 (platelet-endothelial cell adhesion molecule-1, PECAM-1), CD34, CD45 (leukocyte common antigen), CD50 (intercellular adhesion molecule-1, ICAM-1), CD90 (Thy-1), CD117 (c-kit), and CD133. Primary UCBMSCs displayed the same pattern of surface markers as UCB-

TERT-21 cells, implying that the surface marker expression was unaffected by the exogenously expressed hTERT.

Absence of $p16^{INK4a}$ in Parental UCBMSCs

Expression of $p16^{INK4a}$ /RB premature senescence-associated proteins (Figure 3A) and telomere/p53 replicative senescence-associated proteins (Figure 3B) was analyzed in UCBMSCs, UCBTERT-21, and UCBE6E7-20 cells. $p16^{INK4a}$ was not detected in the UCBMSC lanes until the senescence stage; $p16^{INK4a}$ was not detected until PD 53 and started to be expressed in UCBTERT-21 cells at a low level at PD 69, and $p16^{INK4a}$ was detected in UCBE6E7-20 cells at PD 37, immediately before the crisis stage. The protein levels of p53 and p21 in UCBMSCs became up-regulated as the number of PDs increased, but the protein levels of p53 and p21 became down-regulated in UCBE6E7-20 cells, implying that exogenously introduced E6 targets p53 for proteolytic degradation. ATM in UCBE6E7-20 cells was phosphorylated, probably because of DNA damage or telomere length shortening (Figure 3B, lane 8). p53, phosphorylated p53, and p21 were induced by H_2O_2 , a physiological stressor, in UCBTERT-21 cells (Figure 3B, lane 9). The hypophosphorylated forms of

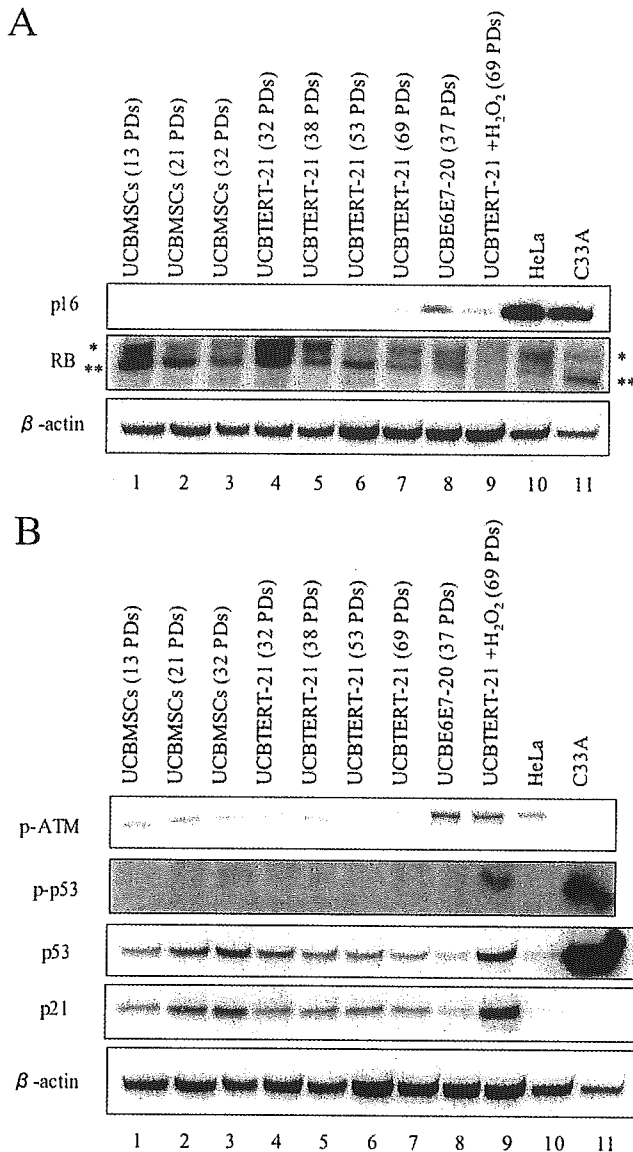


Figure 3. Time-course analysis of cell cycle-associated protein levels in UCBMSCs, UCBE6E7-20 cells, and UCBTERT-21 cells. UCBMSCs, UCBE6E7-20 cells, and UCBTERT-21 cells were analyzed by Western blotting for cell cycle-associated p16^{INK4a}, RB, p-ATM (Ser1981), phospho-p53 (p-p53) (Ser15), p53, p21 and β -actin protein levels. (A) "p16^{INK4a}-RB" senescence (premature senescence) pathway-associated protein levels, i.e., p16^{INK4a} and RB. The hyperphosphorylated and hypophosphorylated forms of RB were indicated as a single asterisk and double asterisks, respectively. (B) Telomere shorten-p53' senescence (replicative senescence) pathway-associated protein levels, i.e., p-ATM, p-p53, p53, and p21. Cells were cultured for the PDs indicated and assayed. Expression of β -actin protein was monitored as a loading control.

RB became dominant and the hyperphosphorylated forms decreased with passage of UCBMSCs (Figure 3A, lanes 1–3), correlating to the increase in p53 and p21 (Figure 3B, lanes 1–3) and to the decrease in cell growth. Transduction of hTERT transiently and markedly increased the hyperphosphorylated form (Figure 3A, lane 4), corresponding to the sudden recovery in proliferation and to a shorter doubling time. Finally, both hyper- and hypophosphorylated forms of RB remained at steady-state levels (Figure 3A, lanes 5–7),

although the hypophosphorylated form seemed dominant at PD 53 (Figure 3A, lane 6), perhaps due to the higher cell density at collection of cell lysate. The protein level of RB was down-regulated in E7-overexpressing UCBE6E7-20 cells (Figure 3A, lane 8), probably as a result of enhanced proteolysis by E7.

Increase in Telomerase Activity and Maintenance of Telomere Length in Cells Transduced with the hTERT

Telomerase activity is revealed by the characteristic six base pair ladder of bands detected by TRAP assay (Figure 4A). No telomerase activity was detected in UCBMSCs at any PDs tested, UCBE6E7-20 cells, UCBMSCs infected with the vector-alone or CHAPS buffer, or mock infected. By contrast, the cells transduced with the hTERT exhibited significant levels of telomerase activity, comparable to HeLa cells as a positive control and to TSR8, which is a synthetic template of eight telomeric repeats used as a polymerase chain reaction (PCR)-positive control.

Average telomere length was longer in the UCBTERT-21 cells than in UCBMSCs. Telomere length in UCBMSCs decreased with the number of PDs, whereas it remained the same in UCBTERT-21 cells, regardless of the number of PDs. The telomere length of UCBE6E7-20 cells was shorter than that of the parental UCBMSCs at senescence.

Normal Diploid Karyotypes with XY Sex Chromosomes in UCBMSCs and UCBTERT-21 Cells

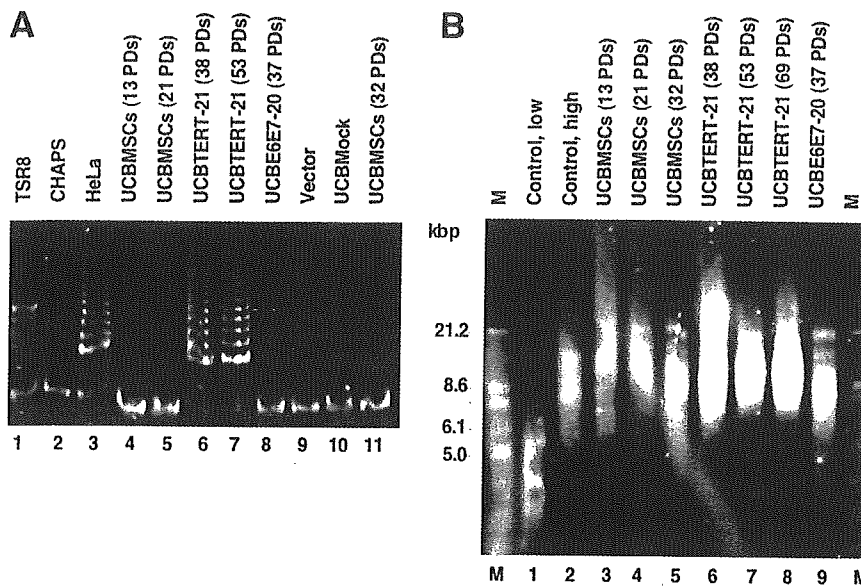
Karyotypic analyses of UCBMSCs were performed at PD 5 (2 passages) and of UCBTERT-21 cells at PD 32 (14 passages). UCBMSCs and UCBTERT-21 cells were found to be diploid and not to exhibit any significant chromosomal abnormalities (Figure 5, A and B). The chromosome number of both UCBMSCs at PD 5 and UCBTERT-21 cells at PD 35 was 46, except for one UCBTERT-21 cell, which contained 47 chromosomes (Figure 5C). No UCBTERT-21 cells containing abnormal numbers of chromosome were found on further analysis. The sex chromosomes were found to be XY, indicating that the cells were of fetal origin.

Osteogenic and Adipogenic Differentiation Potentials of UCBMSCs and UCBTERT-21 Cells

The multipotency of UCBMSCs and UCBTERT-21 cells was assessed by conventional protocols. The osteogenic differentiation potential of UCBMSCs and UCBTERT-21 cells was assessed based on their morphology and von Kossa staining after 3 wk of induction (Figure 6). Multiple small Oil-Red-O-positive fat droplets had accumulated in UCBMSCs and UCBTERT-21 cells after 3 and 2 wk, respectively, of adipogenic induction. Adipocyte differentiation was estimated by counting 2000 cells per dish. The results of triplicate experiments showed that 5.0 and 5.4% of the UCBMSC and UCBTERT-21 cells became positive for fat droplets with Oil-Red stain as a result of adipogenic induction and >90% of the cells were positive on ALP staining after osteogenic induction. We also induced these cells to differentiate into multiple lineages by the methods for neural (Kohyama *et al.*, 2001), cardiomyogenic (Makino *et al.*, 1999; Takeda *et al.*, 2004), and chondrogenic (Imabayashi *et al.*, 2003) lineages; however, the UCBMSC and UCBTERT-21 cells were not induced to differentiate into these lineages in vitro.

DISCUSSION

This study was undertaken to obtain human UCB-derived fetal cells that retain critical cell functions, the same as bone marrow-derived mesenchymal stem cells, mammary gland



irrespective of the number of PDs (lanes 6–8). The telomere length of UCBE6E7-20 cells at PD 37 (lane 9) was shorter than that of the parental UCBMSCs at PD 32 (lane 5). Lanes 1 and 2 are control DNAs of short length and long length, respectively.

Figure 4. Telomerase activity and telomere length of UCBMSCs, UCBE6E7-20 cells, and UCBTERT-21 cells. (A) Analysis of telomerase activity by the PCR assay in UCBMSCs, UCBE6E7-20 cells, and UCBTERT-21 cells. Telomerase activity is revealed by the characteristic six-base pair ladder of bands. No telomerase activity was detected in the UCBMSCs at PD 13, 21, or 32 (lanes 4, 5, and 11, respectively), the UCBE6E7-20 cells at PD 37 (lane 8), the UCBMSCs infected with the vector alone (lane 9), the CHAPS buffer alone (lane 2) or Mock infected cells (lane 10). By contrast, the UCBTERT-21 cells at PD 38 and 53 exhibited significant telomerase activity (lanes 6 and 7, respectively) that was comparable with that of the HeLa cells (lane 3) and TSR8 (lane 1) as positive controls. (B) Telomere length of UCBMSCs, UCBE6E7-20 cells, and UCBTERT-21 cells. Telomere length was longer in the UCBTERT-21 cells than in the parental UCBMSCs. The telomere length of UCBMSCs at PD 13, 21, and 32 decreased as the number of PDs increased (lanes 3–5). The telomere length of UCBTERT-21 cells was maintained, but the telomere length of UCBE6E7-20 cells at PD 37 (lane 9) was shorter than that of the parental UCBMSCs at PD 32 (lane 5).

epithelial cells, skin keratinocytes, and pigmented epithelial cells. It may be possible to use human UCB- and bone marrow-derived stem cells in the future clinically to supply defective enzymes to patients with genetic metabolic diseases, such as neuro-Gaucher disease, Fabry disease, and mucopolysaccharidosis, whose prognosis is poor, and is sometimes lethal. To achieve this, we attempted to prolong the life span of UCB-derived cells or to endow them with immortality without transformation, defining “immortality” simply as indefinite cell division.

Is Successful Prolongation of UCBMSCs Life Span without Inhibition of the $p16^{INK4a}/RB$ Pathway Attributable to a Lack of Ex Vivo Culture Stress?

In contrast to our previous study by using bone marrow-derived cells (Takeda *et al.*, 2004), surprisingly, the successful prolongation of the life span of the UCB-derived fetal cells obtained in this study did not require inhibition of the $p16^{INK4a}/RB$ pathway or premature senescence-associated pathway. Immortalization of some human cell types requires inhibition of the $p16^{INK4a}/RB$ pathway in addition to activation of telomerase (Kiyono *et al.*, 1998; Ishikawa, 2003). Human mammary epithelial cells, endometrial glandular cells, skin keratinocytes, and marrow-derived cells require inhibition of the $p16^{INK4a}/RB$ pathway for immortalization, but foreskin fibroblasts do not. Activation of telomerase alone is sufficient for immortalization of human foreskin fibroblasts. HPV16 E6 and E7 have been used to inhibit p53 and RB, respectively, to prolong the life span of marrow-derived MSCs (Okamoto *et al.*, 2002; Takeda *et al.*, 2004), endometrial gland cells (Kyo *et al.*, 2003), mammary epithelial cells, and keratinocytes (Kiyono *et al.*, 1998). Bmi-1 also has been used to inhibit $p16^{INK4a}$ transcription to prolong the life span of marrow-derived MSCs. One function of this $p16^{INK4a}$ protein is to maintain pRB in a hypophosphorylated active form, which inhibits cell cycle progression.

Our present findings that UCB-derived cells can be immortalized without inhibition of the $p16^{INK4a}/RB$ pathway is consistent with the results in regard to foreskin fibroblasts. This successful immortalization of UCB-cells by hTERT

alone can be explained by lack of ex vivo culture stress under the culture condition used in this study. Alternatively, only cells insensitive to ex vivo culture stress or lacking $p16^{INK4a}$ induction may be expanded by hTERT alone. Primary UCB-derived cell culture succeeded in 94% of the attempts (15 of 16 trials), and the cells were passaged only two or three times before reaching premature senescence (13 of 15 primary UCB-derived cell cultures); however, only two cell strains (UCBMSCs) were established from them (2 of 15 primary UCB-derived cell cultures; see *Materials and Methods*. “Isolation and Cell Culture of UCBMSCs”). Based on the results of this study by using one of the two cell strains, the establishment of these strains (UCBMSCs) can be explained by 1) lack of $p16^{INK4a}$ in primary cultured UCB-derived cells or 2) selection of cells that do not express $p16^{INK4a}$ from a heterogeneous population. We cannot exclude either possibilities, and we did observe two different types of cells, i.e., rapidly growing cells and quiescent cells in the primary culture of cord blood cells. If the alternative explanation is true, these quiescent cells, in which $p16^{INK4a}$ may be expressed at a high level, can be efficiently expanded by introduction of E7, the inhibitor of RB, or Bmi-1, the down-regulator of $p16^{INK4a}$. We also performed additional experiments by using newly obtained specimens from umbilical cord to determine whether infection of the primary or first passage cells generates long-term strains routinely and efficiently. We generated other cells, UCB408 cells, and found that generation of long-term strains was reproducible (Supplementary Figure A). The UCBE6E7-31 and UCBE7-32 cells proliferated for >30 PDs and exhibited persistent growth. The UCBTERT-30 cells exhibited a prolonged cell life span in culture and reached PD 19, but they failed to be immortalized. The success of immortalization of UCBMSCs may still be low, probably due to expression of $p16^{INK4a}$ premature senescence-associated proteins in the early passage of the UCB408 cells. Because the 5' CpG island of the $p16^{INK4a}$ promoter based on published genome sequences (GenBank accession no. AF022809, U12818, and AC000048) has been found to be methylation-free by the bisulfite method (Supplementary Figures B and C), the lack of

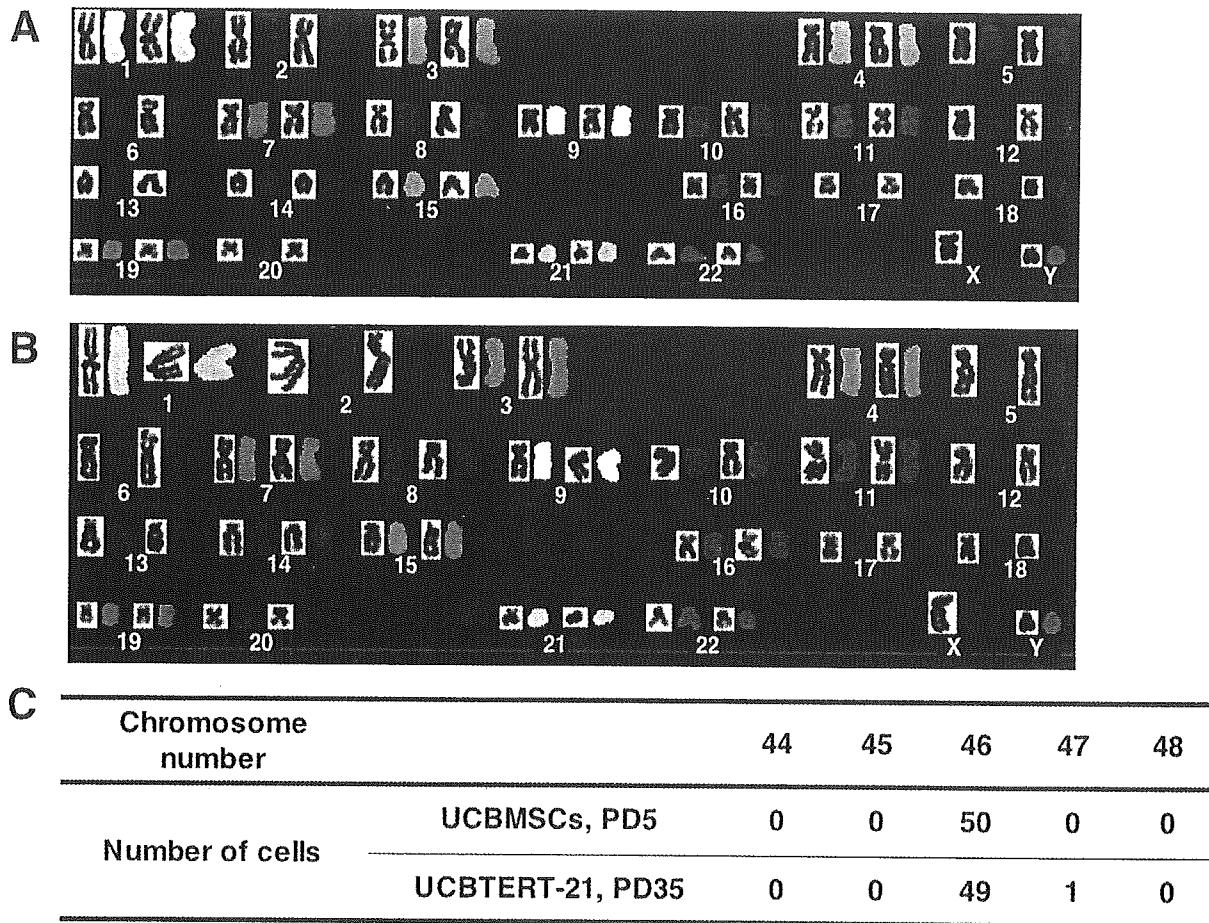


Figure 5. Karyotypic analysis of UCBMSCs and UCBTERT-21 cells. Comprehensive karyotyping (left side, reverse DAP, right side, SKY), UCBMSCs at PD 5 (A) and UCBTERT-21 cells at PD 35 (B). Normal diploidy is seen in the UCBMSCs and UCBTERT-21 cells. Both cells were analyzed for chromosome number (C). None of the 50 UCBMSCs tested showed any abnormal numbers of chromosomes. Of the 50 UCBTERT-21 cells tested, 49 exhibited normal diploidy and one cell contained 47 chromosomes. No UCBTERT-21 cells with an abnormal chromosome number were found on further analysis.

p16^{INK4a} expression in rapidly growing cells is not due to methylation of the p16^{INK4a} promoter, unlike human mammary epithelial cells (Umezawa *et al.*, 1997; Foster *et al.*, 1998; Wong *et al.*, 1999).

UCB-derived Cells Are of Mesenchymal Origin

The differentiation capacity of UCB-derived cells was unaffected during establishment of a plate-adhering population of cells from UCB. The cells established from UCB can be extensively and clonally expanded in vitro while retaining their potential to differentiate into osteoblasts that produce mineralized matrices and adipocytes that accumulate lipid vacuoles under in vitro conditions. This differentiation potential of the UCB-derived cells is the same as that reported for bone marrow MSCs (Goodwin *et al.*, 2001; Lee *et al.*, 2004).

The surface markers of the UCB-derived cells examined in this study are exactly the same as those of previously reported UCB-derived cells (Lee *et al.*, 2004). Most of the surface markers are the same as those detected in their bone marrow counterparts (Takeda *et al.*, 2004), with both UCB- and bone marrow-derived cells being positive for CD29, CD44, CD55, and CD59, and negative for CD34 and CD117. The CD90 and CD133 markers, on the other hand, can be used to distinguish UCB-derived cells from bone marrow-derived cells, because they are both expressed in multipo-

tent marrow-derived cells (Takeda *et al.*, 2004) and not in UCB-derived cells (Figure 2) (Lee *et al.*, 2004).

This technique allows the applications of UCB to be further extended and permits it to be used as an alternative to bone marrow as a source of hMSCs; however, this study puts the controversy to rest and substantiates that UCB does contain hMSCs. We believe that the "UCBMSCs" are mesenchymal stem cells derived from UCB, as designated. However, it is difficult to exclude the possibility that the UCBMSCs were derived from mesenchymal cells embedded in the Wharton's jelly of the umbilical cord during insertion of the needle into the vessels through the umbilical cord.

Can primary UCB-derived cell "culture" contribute to cell-based therapy or regenerative medicine? The problems involved in cell-based therapy with human UCB-derived cells are the finite cell life span of the cells and the difficulty of obtaining a large enough number of cells. The technique that allows human cells to escape senescence used in this study may be used to obtain a large number of cells and to overcome these problems of a short life span.

ACKNOWLEDGMENTS

We thank members of Virology Division, National Cancer Center Research Institute (Tokyo, Japan) for helpful discussion and continuous encouragement

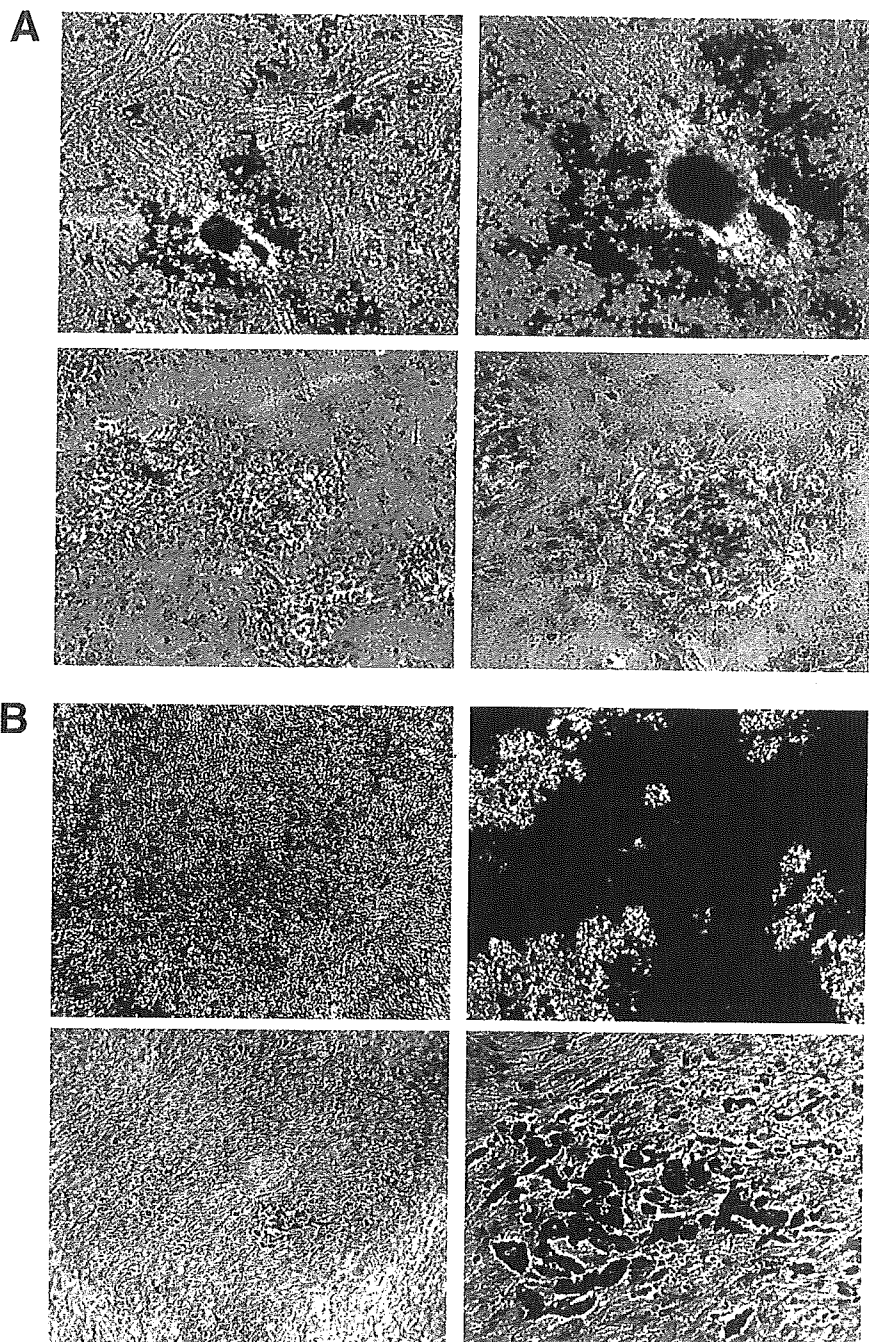


Figure 6. Osteogenic and adipogenic differentiation of UCBMSCs and UCBTERT-21 cells. UCBMSCs (A) and UCBTERT-21 cells (B) were examined by von Kossa staining after 3 wk of osteogenic induction (A and B, top columns) and by Oil-Red-O staining after 2 wk of adipogenic induction (A and B, bottom columns). Both cells contained small lipid vacuoles in their cytoplasm. Original magnifications: (A) left column, 10 \times ; right column, 20 \times ; (B) left column, 5 \times ; right column, 20 \times .

of this research. This study was supported by a grant from the Ministry of Education, Culture, Sports, Science, and Technology (MEXT) of Japan and the Health and Labor Sciences Research grants (to A. U. and T. K.); the Pharmaceuticals and Medical Devices Agency (to A. U.); an Award for Research Resident Fellowship from the Japan Health Sciences Foundation (to M. T.); and the Japan Association for the Advancement of Medical Equipment (to T. U.).

REFERENCES

Blackburn, E. H. (2000a). Telomere states and cell fates. *Nature* 408, 53–56.
 Blackburn, E. H. (2000b). Telomeres and telomerase. *Keio J. Med.* 49, 59–65.
 Blackburn, E. H. (2001). Switching and signaling at the telomere. *Cell* 106, 661–673.

Burk, R. D., *et al.* (2003). Distribution of human papillomavirus types 16 and 18 variants in squamous cell carcinomas and adenocarcinomas of the cervix. *Cancer Res.* 63, 7215–7220.

Campisi, J. (1997). The biology of replicative senescence. *Eur. J. Cancer* 33, 703–709.

Caplan, A. I. (1991). Mesenchymal stem cells. *J. Orthop. Res.* 9, 641–650.

Caplan, A. I., and Bruder, S. P. (2001). Mesenchymal stem cells: building blocks for molecular medicine in the 21st century. *Trends Mol. Med.* 7, 259–264.

D’Ippolito, G., Schiller, P. C., Ricordi, C., Roos, B. A., and Howard, G. A. (1999). Age-related osteogenic potential of mesenchymal stromal stem cells from human vertebral bone marrow. *J. Bone Miner. Res.* 14, 1115–1122.

Dimri, G. P., *et al.* (1995). A biomarker that identifies senescent human cells in culture and in aging skin in vivo. *Proc. Natl. Acad. Sci. USA* 92, 9363–9367.

- Foster, S. A., Wong, D. J., Barrett, M. T., and Galloway, D. A. (1998). Inactivation of p16 in human mammary epithelial cells by CpG island methylation. *Mol. Cell. Biol.* 18, 1793–1801.
- Gewin, L., Myers, H., Kiyono, T., and Galloway, D. A. (2004). Identification of a novel telomerase repressor that interacts with the human papillomavirus type-16 E6/E6-AP complex. *Genes Dev.* 18, 2269–2282.
- Goodwin, H. S., Bicknese, A. R., Chien, S. N., Bogucki, B. D., Quinn, C. O., and Wall, D. A. (2001). Multilineage differentiation activity by cells isolated from umbilical cord blood: expression of bone, fat, and neural markers. *Biol. Blood Marrow Transplant* 7, 581–588.
- Hayflick, L. (1976). The cell biology of human aging. *N. Engl. J. Med.* 295, 1302–1308.
- Imabayashi, H., Mori, T., Gojo, S., Kiyono, T., Sugiyama, T., Irie, R., Isogai, T., Hata, J., Toyama, Y., and Umezawa, A. (2003). Redifferentiation of dedifferentiated chondrocytes and chondrogenesis of human bone marrow stromal cells via chondrosphere formation with expression profiling by large-scale cDNA analysis. *Exp. Cell Res.* 288, 35–50.
- Ishikawa, F. (2003). Cellular senescence, an unpopular yet trustworthy tumor suppressor mechanism. *Cancer Sci.* 94, 944–947.
- Jaiswal, N., Haynesworth, S. E., Caplan, A. I., and Bruder, S. P. (1997). Osteogenic differentiation of purified, culture-expanded human mesenchymal stem cells in vitro. *J. Cell. Biochem.* 64, 295–312.
- Jiang, Y., *et al.* (2002). Pluripotency of mesenchymal stem cells derived from adult marrow. *Nature* 418, 41–49.
- Kiyono, T., Foster, S. A., Koop, J. I., McDougall, J. K., Galloway, D. A., and Klingelhutz, A. J. (1998). Both Rb/p16^{INK4a} inactivation and telomerase activity are required to immortalize human epithelial cells. *Nature* 396, 84–88.
- Kohyama, J., Abe, H., Shimazaki, T., Koizumi, A., Nakashima, K., Gojo, S., Taga, T., Okano, H., Hata, J., and Umezawa, A. (2001). Brain from bone: efficient “meta-differentiation” of marrow stroma-derived mature osteoblasts to neurons with Noggin or a demethylating agent. *Differentiation* 68, 235–244.
- Kyo, S., Nakamura, M., Kiyono, T., Maida, Y., Kanaya, T., Tanaka, M., Yatabe, N., and Inoue, M. (2003). Successful immortalization of endometrial glandular cells with normal structural and functional characteristics. *Am. J. Pathol.* 163, 2259–2269.
- Lee, O. K., Kuo, T. K., Chen, W. M., Lee, K. D., Hsieh, S. L., and Chen, T. H. (2004). Isolation of multipotent mesenchymal stem cells from umbilical cord blood. *Blood* 103, 1669–1675.
- Makino, S., *et al.* (1999). Cardiomyocytes can be generated from marrow stromal cells in vitro. *J. Clin. Invest.* 103, 697–705.
- Mayani, H., and Lansford, P. M. (1998). Biology of human umbilical cord blood-derived hematopoietic stem/progenitor cells. *Stem Cells* 16, 153–165.
- Okamoto, T., Aoyama, T., Nakayama, T., Nakamata, T., Hosaka, T., Nishijo, K., Nakamura, T., Kiyono, T., and Toguchida, J. (2002). Clonal heterogeneity in differentiation potential of immortalized human mesenchymal stem cells. *Biochem. Biophys. Res. Commun.* 295, 354–361.
- Owen, M. (1988). Marrow stromal stem cells. *J. Cell Sci. Suppl.* 10, 63–76.
- Pittenger, M. F., Mackay, A. M., Beck, S. C., Jaiswal, R. K., Douglas, R., Mosca, J. D., Moorman, M. A., Simonetti, D. W., Craig, S., and Marshak, D. R. (1999). Multilineage potential of adult human mesenchymal stem cells. *Science* 284, 143–147.
- Prockop, D. J. (1997). Marrow stromal cells as stem cells for nonhematopoietic tissues. *Science* 276, 71–74.
- Prockop, D. J., Sekiya, I., and Colter, D. C. (2001). Isolation and characterization of rapidly self-renewing stem cells from cultures of human marrow stromal cells. *Cytotherapy* 3, 393–396.
- Sasaki, M. S. (1975). A comparison of chromosomal radiosensitivities of somatic cells of mouse and man. *Mutat. Res.* 29, 433–448.
- Sekiguchi, T., and Hunter, T. (1998). Induction of growth arrest and cell death by overexpression of the cyclin-Cdk inhibitor p21 in hamster BHK21 cells. *Oncogene* 16, 369–380.
- Sekiguchi, T., Nishimoto, T., and Hunter, T. (1999). Overexpression of D-type cyclins, E2F-1, SV40 large T antigen and HPV16 E7 rescue cell cycle arrest of tsBN462 cells caused by the CCG1/TAF(II)250 mutation. *Oncogene* 18, 1797–1806.
- Sekiya, I., Larson, B. L., Vuorio, J. T., Cui, J. G., and Prockop, D. J. (2004). Adipogenic differentiation of human adult stem cells from bone marrow stroma (MSCs). *J. Bone Miner. Res.* 19, 256–264.
- Takeda, Y., *et al.* (2004). Can the life span of human marrow stromal cells be prolonged by bmi-1, E6, E7, and/or telomerase without affecting cardiomyogenic differentiation? *J. Gene Med.* 6, 833–845.
- Tsuchiya, K., Mori, T., Chen, G., Ushida, T., Tateishi, T., Matsuno, T., Sakamoto, M., and Umezawa, A. (2004). Custom-shaping system for bone regeneration by seeding marrow stromal cells onto a web-like biodegradable hybrid sheet. *Cell Tissue Res.* 316, 141–153.
- Umezawa, A., Maruyama, T., Segawa, K., Shaddock, R. K., Waheed, A., and Hata, J. (1992). Multipotent marrow stromal cell line is able to induce hematopoiesis in vivo. *J. Cell. Physiol.* 151, 197–205.
- Umezawa, A., Yamamoto, H., Rhodes, K., Klemsz, M. J., Maki, R. A., and Oshima, R. G. (1997). Methylation of an ETS site in the intron enhancer of the keratin 18 gene participates in tissue-specific repression. *Mol. Cell. Biol.* 17, 4885–4894.
- Vaziri, H., Dragowska, W., Allsopp, R. C., Thomas, T. E., Harley, C. B., and Lansford, P. M. (1994). Evidence for a mitotic clock in human hematopoietic stem cells: loss of telomeric DNA with age. *Proc. Natl. Acad. Sci. USA* 91, 9857–9860.
- Wong, D. J., Foster, S. A., Galloway, D. A., and Reid, B. J. (1999). Progressive region-specific de novo methylation of the p16 CpG island in primary human mammary epithelial cell strains during escape from M(0) growth arrest. *Mol. Cell. Biol.* 19, 5642–5651.